Conformations and Infrared Spectra of α-Oxo Ketenes from *ab Initio* Calculations: The Role of Electrostatics

David M. Birney

The Department of Chemistry and Biochemistry, Texas Tech University, Lubbock, Texas 79409-1061

Received September 14, 1993 (Revised Manuscript Received February 16, 1994•)

The *Z* and *E* conformations of acetylketene (3) and its 2-methyl- and 2-chloro derivatives (6 and 8, respectively) have been obtained using *ab initio* molecular orbital theory at the RHF/6-31G* level, while formylketene (12) was studied at the MP2/6-31G* level. Comparison of the calculated IR spectra (RHF/6-31G*) with the experimental spectra aids in the assignment of observed absorptions, provides an estimate of the *Z*/*E* ratio, and offers an explanation of trends in the IR spectra. The relative energies were calculated at the MP2 through MP4(SDQ)/6-31G* levels, all of which predict that the *Z* conformations of 3 and 8 are more stable, while the *E* conformation of 6 is favored, in quantitative agreement with experiment. The underlying preference for the *Z* conformation is due to an electrostatic attraction between the carbonyl oxygen and the central carbon of the ketene. However, steric and entropic effects combine to make *E* the preferred conformation of 6.

Introduction

α-Oxo ketenes have been implicated as or demonstrated to be intermediates in a variety of reactions.[1] The observation that the characteristic reactivities of these synthetically useful molecules are often different from those of ketene itself has recently prompted a number of mechanistic[1g,l] and theoretical studies.[2] Matrix isolation and infrared spectroscopy have been used to trap and identify a variety of α-oxo ketenes, including 3,[1g,p] 6,[1k] and 8.[3] These were prepared by a number of routes, illustrated in Scheme 1, including the pyrolysis of β-keto esters,[1i,j,l,p] the fragmentation of 4*H*-1,3-dioxin-4-ones,[1j,3] the deazetization or α-aza-β-diketones[1p] and the decarbonylation of furandiones.[1m,n] The latter three processes occur both thermally and photochemically. Steric hindrance reduces the reactivity of dipivaloylketene (10) sufficiently that it is stable in solution at 0 °C and the X-ray crystal structure of its dimer 11, which is itself an α-oxo ketene, has been obtained.[1m,n]

There are two conformations of α-oxo ketenes, *Z* and *E*. The equilibrium mixture generated by pyrolysis can often be trapped and observed under argon matrix isolation conditions while photolysis in a matrix may give a single conformation. Flash vacuum pyrolysis of 2, in equilibrium with 1, gives both (*Z*)- and (*E*)-3,[1k] while photolysis of 4 gives only one of the conformations, assigned as the *Z*,[1k] and in addition, an unidentified photoproduct. Pyrolysis of methyl 2-methyl-3-oxobutanoate gives primarily one conformation (*E*) of 6 while photolysis of 5 gives exclusively (*E*)-6.[1p] Pyrolysis of 7 gives 8, again as a mixture of *Z* and *E*.[3] The steric crowding in dipivaloylketene (10), formed by photochemical extrusion of CO from 9, lends it stability in solution at 0 °C.[1m,n] The X-ray structure of the even more congested dimer 11 shows a *Z* conformation for the α-oxo ketene functionality.[1m,n] The conformational preference is clearly sensitive to the substitution. Steric crowding has been suggested as the origin of the *E*

Scheme 1

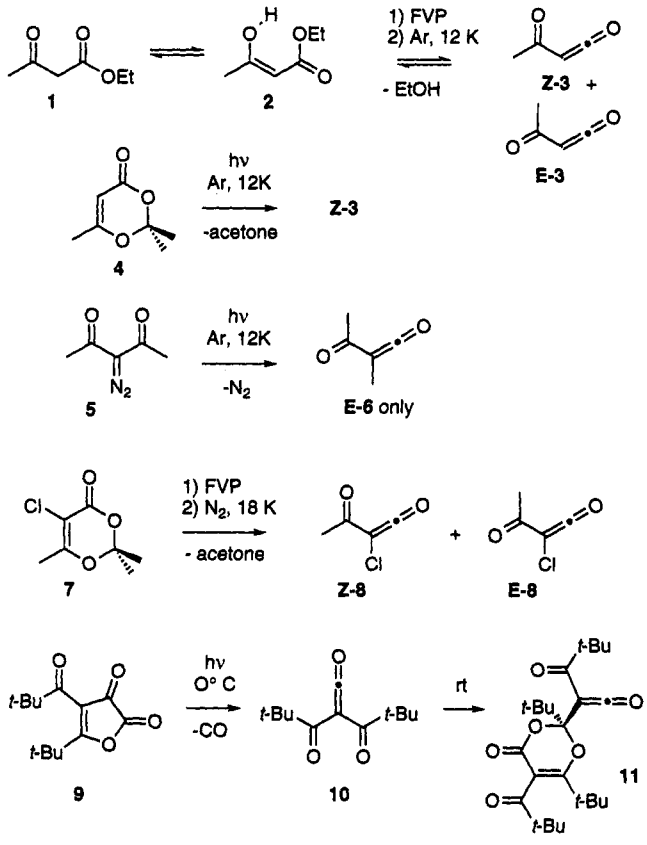

• Abstract published in *Advance ACS Abstracts*, April 1, 1994.

(1) (a) Newman, M. S.; Zuech, E. A. *J. Org. Chem.* **1962**, *27*, 1436. (b) Jager, G. *Chem. Ber.* **1965**, *98*, 1184. (c) Ulrich, H. *Cycloaddition Reactions of Heterocumulenes*; Academic Press: New York, 1967; Vol. 9, pp 38–109. (d) Ghosez, L.; O'Donnell, M. J. In *Pericyclic Reactions*; Marchand, A. P., and Lehr, R. E., Eds.; Academic Press: New York, 1977; Vol. 2; pp 79–141. (e) Nikolaev, V. A.; Frenkh, Y.; Korobitsyna, I. K. *J. Org. Chem. USSR (Eng. Transl.)* **1978**, *14*, 1069–1079. (f) Hyatt, J. A.; Feldman, P.; Clemens, R. J. *J. Org. Chem.* **1984**, *49*, 5105–5108. (g) Clemens, R. J.; Witzeman, J. S. *J. Am. Chem. Soc.* **1989**, *111*, 2186–2193. (h) Kaneko, C.; Sato, M.; Sakaki, J.-i.; Abe, Y. *J. Heterocycl. Chem.* **1990**, *27*, 25. (i) Witzeman, J. S. *Tetrahedron Lett.* **1990**, *31*, 1401–1404. (j) Witzeman, J. S.; Nottingham, W. D. *J. Org. Chem.* **1991**, *56*, 1713–1718. (k) Freiermuth, B.; Wentrup, C. *J. Org. Chem.* **1991**, *56*, 2286–2289. (l) Emerson, D. W.; Titus, R. L.; Gonzales, R. M. *J. Org. Chem.* **1991**, *56*, 5301. (m) Kappe, C. O.; Evans, R. A.; Kennard, C. H. L.; Wentrup, C. *J. Am. Chem. Soc.* **1991**, *113*, 4234–4237. (n) Kappe, C. O.; Farber, G.; Wentrup, C.; Kollenz, G. *J. Org. Chem.* **1992**, *57*, 7078–7083. (o) Leung-Toung, R.; Wentrup, C. *Tetrahedron* **1992**, *48*, 7641–7654. (p) Leung-Toung, R.; Wentrup, C. *J. Org. Chem.* **1992**, *57*, 4850–4858. (q) Coleman, R. S.; Fraser, J. R. *J. Org. Chem.* **1993**, *58*, 385–392.

(2) (a) Allen, A. D.; Gong, L.; Tidwell, T. T. *J. Am. Chem. Soc.* **1990**, *112*, 6396–6397. (b) Nguyen, M. T.; Ha, T.; More O'Ferrall, R. A. *J. Org. Chem.* **1990**, *55*, 3251–3256. (c) Gong, L.; McAllister, M. A.; Tidwell, T. T. *J. Am. Chem. Soc.* **1991**, *113*, 6021–6028. (d) Birney, D. M.; Wagenseller, P. E. *J. Am. Chem. Soc.*, submitted.

(3) Witzeman, J. S. Personal communication.

0022-3263/94/1959-2557$04.50/0

preference of **6** and **11**.[1m,n,p] No explanation has been offered for the apparent underlying preference for the *Z* conformation. The assignment of *Z* and *E* conformations is based on the infrared spectra and relies in particular on the fact that the separations between the ketene and carbonyl stretches in *Z* conformations are greater than in *E* (see Table 5). Despite its importance to the structural assignments, no explanation of this trend has been advanced.

There have been several calculations reported on α-oxo ketenes. Although the simplest species, formylketene (**12**), has not been observed, Nguyen, Ha, and More O'Ferrall[2b] have studied its hypothetical ring closure to **13** (eq 1) using

12 ⇌ **13** (1)

ab initio methods. Their results (MP4(SDQ)/6-31G**//RHF/6-31G** + ZPE) indicate that the *Z* form is slightly stabilized (0.2 kcal/mol) relative to the *E*, but they do not discuss the origin of this preference nor do they report the IR spectra of the conformations. Allen, Gong, and Tidwell have performed RHF/3-21G calculations on formylketene.[2a] They report that isodesmic reactions indicate that the formyl substituent stabilizes ketene by 3.3 kcal/mol, but do not discuss the molecule further. Other work from this laboratory has examined the reactivity of formylketene (**12**) with geometry optimization at the MP2/6-31G* level but has not addressed the conformational preferences.[2d]

Freiermuth and Wentrup report MNDO calculations on **3** which predict the *Z* conformation is more stable by 2.7 kcal/mol, in only qualitative agreement with the experimental preference.[1k] They also report that the calculated IR spectra predict the *Z* ketene stretch to be at slightly higher frequency than the *E* form, again in qualitative agreement with experiment.

This *ab initio* molecular orbital study of α-oxo ketenes was undertaken with the anticipation that effects of the substituent would elucidate the factors contributing to the varying conformational preferences of the species. Furthermore, since the primary method used for the detection of these intermediates has been IR spectroscopy, the calculated vibrational spectra were expected to prove useful for confirming the identities of the matrix species and aid in making further peak assignments. The calculated IR intensities would also be useful for quantifying the proportions of *Z* and *E* conformers of each spectrum, thus allowing the determination of the equilibrium concentrations.

Computational Methods

The *ab initio* calculations were carried out with GAUSSIAN 88, 90, and 92,[4] and using standard basis sets. Structures were optimized in C_s symmetry at both the RHF/3-21G and RHF/6-31G* levels using standard gradient techniques. The structures obtained are shown in Figure 1 and were confirmed as minima by frequency calculations. Selected geometrical parameters are reported in Table 1; the complete optimized *Z*-matrices are included in the supplementary material. The effects of electron correlation on the vibrational frequencies was examined by frequency calculations on formylketene (**12**)[2d,5] using second-order Moller–Plesset perturbation theory (MP2) with the 6-31G* basis set. Single point energy calculations were carried out on all structures at the MP2, MP3, MP4(DQ), and MP4(SDQ) levels at the highest level geometry. Total energies are reported in Table 2, and relative energies of *Z* and *E* conformers are reported in Table 3. Atomic charges are reported in Table 4. In addition to those from the Mulliken analysis, charges were obtained using the natural bond orbital analysis[6] method and using the CHELPG program.[7] The latter evaluates the electrostatic potential

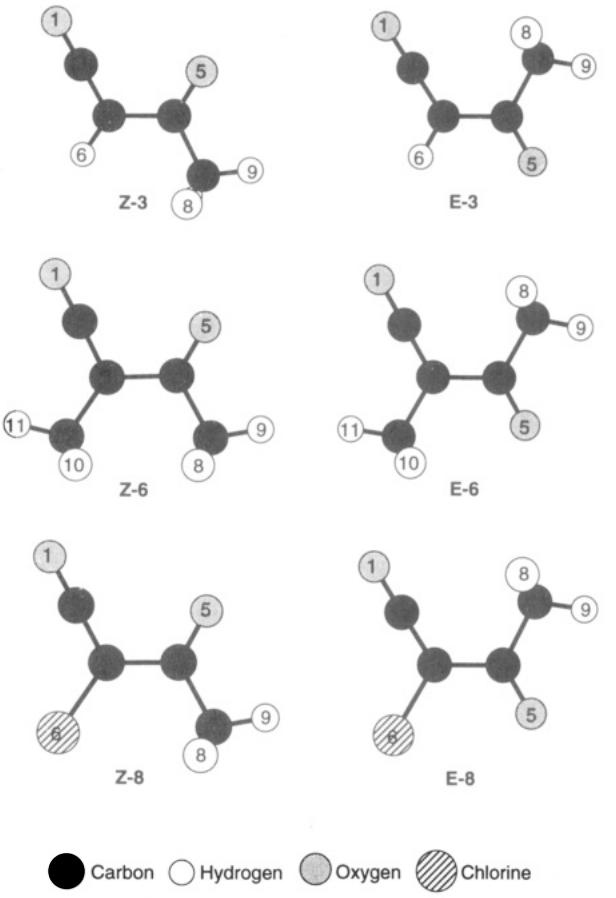

Figure 1. Calculated geometries of (*Z*)- and (*E*)-**3**, **6**, and **8** obtained at the RHF/6-31G* level.

Table 1. Selected Geometrical Parameters of Acetylketene and Derivatives[a]

	3		6		8	
parameter	*Z*	*E*	*Z*	*E*	*Z*	*E*
$r(O_1–C_2)$[b]	1.133	1.138	1.136	1.141	1.131	1.136
$r(C_2–C_3)$[b]	1.324	1.318	1.325	1.317	1.328	1.321
$r(C_3–C_4)$[b]	1.471	1.476	1.475	1.478	1.475	1.481
$r(C_4–O_5)$[b]	1.198	1.194	1.200	1.196	1.197	1.189
$\angle(O_1–C_2–C_3)$[c,d]	179.2	179.9	178.5	179.8	179.2	179.4
$\angle(C_2–C_3–C_4)$[c]	118.3	123.3	114.4	119.8	117.4	122.3
$\angle(C_3–C_4–O_5)$[c]	121.9	120.1	121.4	118.9	119.0	120.7
$\angle(C_2–C_3–X_6)$[c,e]	117.7	117.3	119.9	120.6	117.7	117.0
$\angle(C_4–C_3–X_6)$[c,e]	124.0	119.4	125.7	119.6	124.9	120.6
$\angle(C_3–C_4–C_7)$[c]	115.8	118.2	117.0	118.9	118.0	116.9

[a] Geometries were optimized at the RHF/6-31G* level. [b] Angstroms. [c] Degrees. [d] In all cases the ketene bends away from the acetyl group; i.e., the $O_1–C_3–C_4$ angle is larger than the $C_2–C_3–C_4$ angle. [e] X = H for **3**, X = C for **6**, X = Cl for **8**.

(4) (a) Gaussian 90: Frisch, M. J.; Head-Gordon, M.; Trucks, G. W.; Foresman, J. B.; Schlegel, H. B.; Raghavachari, K.; Robb, M.; Binkley, J. S.; Gonzalez, C.; Defrees, D. J.; Fox, D. J.; Whiteside, R. A.; Seeger, R.; Melius, C. F.; Baker, J.; Martin, R. L.; Kahn, L. R.; Stewart, J. J. P.; Topiol, S.; Pople, J. A. Gaussian, Inc., Pittsburgh, PA, 1990. (b) Gaussian 92: Frisch, M. J.; Trucks, G. W.; Head-Gordon, M.; Gill, P. M. W.; Wong, M. W.; Foresman, J. B.; Johnson, B. G.; Schlegel, H. B.; Robb, M. A.; Replogle, E. S.; Gomperts, R.; Andres, J. L.; Raghavachari, K.; Binkley, J. S.; Gonzalez, C.; Martin, R. L.; Fox, D. J.; Defrees, D. J.; Baker, J.; Stewart, J. J. P.; Pople, J. A. Gaussian, Inc., Pittsburgh, PA, 1992.

(5) I thank a reviewer for suggesting this calculation.

Table 2. Energies and Selected Thermodynamic Values of Acetylketene and Derivatives[a]

	3		6		8	
parameter	*Z*	*E*	*Z*	*E*	*Z*	*E*
RHF/3-21G[b,c]	-301.801 43	-301.797 43	-340.619 82	-340.620 42	-758.499 14	-758.495 07
RHF/6-31G*[c]	-303.503 96	-303.501 06	-342.536 87	-342.537 76	-762.387 92	-762.383 99
MP2/6-31G*[c]	-304.349 34	-304.347 91	-343.516 01	-343.518 33	-763.366 03	-763.363 72
MP3/6-31G*[c]	-304.359 94	-304.358 67	-343.534 62	-343.536 87	-763.381 87	-763.379 52
MP4(DQ)/6-31G*[c]	-304.365 43	-304.363 77	-343.541 08	-343.542 87	-763.387 50	-763.384 89
MP4(SDQ)/6-31G*[c]	-304.379 46	-304.378 00	-343.556 38	-343.558 42	-763.402 91	-763.400 42
ZPE[d,e]	48.0	47.9	67.1	67.0	42.2	42.0
S[d,f]	78.3	79.0	85.4	87.1	84.5	86.5
μ (D)	3.84	2.18	4.23	1.78	2.34	3.14

[a] At the RHF/6-31G*-optimized geometry. [b] At the RHF/3-31G-optimized geometry. [c] Hartrees. [d] Unscaled. [e] Zero point energy in kcal/mol. [f] Entropy in cal/mol × K.

Table 3. Relative Energies, Entropies, and Populations of *E* versus *Z* Conformations of Acetylketene and Derivatives

	E versus *Z*				
level of theory	3[a]	6[a]	8[a]	12[b]	12[c]
RHF/3-21G[d,e]	2.5	-0.4	2.6		
RHF/6-31G*[d]	1.8	-0.6	2.5	0.9	
MP2/6-31G*[d]	0.9	-1.5	1.4	0.5	0.5
MP3/6-31G*[d]	0.8	-1.4	1.5	0.3	0.2
MP2(DQ)/6-31G*[d]	1.0	-1.1	1.6		0.5
MP4(SDQ)/6-31G*[d]	0.9	-1.3	1.6	0.5	0.4
MP4 with ZPE[d,f]	0.8	-1.4	1.4	0.2	0.3[g]
ΔS	0.7	1.7	2.0		0.1[g]
pyrolysis temp (°C)	350	700	180		180[h]
Z population at pyrolysis temp (%)	58	18	66		57[h]
est *Z*-population[i] (%)	52[j]	*k*	64[l]		

[a] At RHF/6-31G*-optimized geometries. [b] With the 6-31G** basis set at the RHF geometries from ref 2b. [c] At MP2(full)/6-31G* geometries, from ref 2d. [d] Relative energy in kcal/mol. A positive energy indicates that the *Z* conformation is more stable. [e] At RHF/3-31G-optimized geometries. [f] MP4(SDQ)/6-31G* energies with zero-point energy corrections (scaled by 0.9) from RHF/6-31G* frequencies. [g] ZPE from MP2/6-31G* frequency calculation. [h] For comparison only; formylketene (12) has not been observed experimentally. [i] From experimental intensities of the indicated IR absorption, corrected by the calculated (RHF/6-31G*) intensities from Table 5. [j] Based on the absorptions from ref 11. [k] *E* is reported as strong, *Z* as weak. Reference 1p. [l] Based on the carbonyl adsorption from ref 3.

calculated at a grid of points around a molecule and fits charges to that potential. The electrostatic potential was sampled over a grid extending 2.8 Å beyond the molecule, sampling points were 0.3 Å apart and the exclusion radii employed were 1.50 Å for C, 1.70 Å for O, 1.45 Å for H, and 1.80 Å for Cl as recommended by Breneman and Wiberg.[7]

Results and Discussion

Conformational Preferences. The relative energies of the *Z* and *E* conformations of **3**, **6**, **8**, and **12** are shown in Table 3. The various levels of theory are in qualitative agreement in predicting that the energies of the *Z* conformations of **3**, **8**, and **12** are lower than the *E* conformations, while the preference is reversed for **6**. This trend is consistent with the experimental result that pyrolysis of methyl 2-methyl-3-oxobutanoate gives primarily (*E*)-**6**[1p] while both *Z* and *E* forms of **3**[1k] and **8**[3] are formed in the pyrolyses of **1** and **7**, respectively. Closer examination of the RHF results with both the 3-21G and 6-31G* basis sets shows that they are biased toward the *Z* conformation, as compared to the MP results. At the RHF/6-31G* level, the *Z* forms of **3** and **8** are favored by 1.8 and 2.5 kcal/mol, respectively. In contrast, at the MP4(SDQ)/6-31G* + ZPE level, (*Z*)-**3** and (*Z*)-**8** remain more stable than the *E* forms, but by only 0.8 and 1.4 kcal/mol, respectively. The RHF/6-31G* level also underestimates the relative stability of (*E*)-**6**, finding it only 0.6 kcal/mol more stable than the *Z*, whereas the MP4(SDQ)/6-31G* + ZPE level finds it to be 1.4 kcal/mol more stable than the *Z*. On the other hand, single point calculations with the 6-31G* basis set at the several Møller–Plesset levels (MP2 through MP4(SDQ)) all predict similar *Z*-*E* energy differences. MP4(DQ)/6-31G* favors the *Z* form of **3**, **6**, **8**, and **12** slightly more than the MP2, MP3, or MP4(SDQ) levels, but there is at most a 0.4 kcal/mol variation among the calculated *Z*-*E* energy differences at the various MP levels. Furthermore, the relative energies of (*Z*)-**12** and (*E*)-**12** are essentially unchanged regardless of whether the geometry was optimized at the RHF/6-31G* or MP2/6-31G* level. This suggests there would be no significant advantage to geometry optimization of **3**, **6**, and **8** beyond the RHF/6-31G* level. The entropy difference between the two forms, calculated from the RHF/6-31G* vibrational frequencies, favors the *E* conformation for all three substituted ketenes **3**, **6**, and **8**.

Freezing the products from flash vacuum pyrolysis in a matrix in principle traps the equilibrium population of conformers formed in the pyrolysis, thus measuring Δ*G*. Therefore, Δ*H* and Δ*S* for the two conformations were derived from the calculated energy differences at the MP4/6-31G*//RHF/6-31G* level and the vibrational frequencies from the RHF/6-31G* optimization. The free energy differences (Δ*G*) calculated at the experimental pyrolysis temperatures predict 58% (*Z*)-**3** at 350 °C and similar proportions, 66% (*Z*)-**8** at 180 °C, and 57% (*Z*)-**12** also at 180 °C, in qualitative agreement with the experimental observation of both conformers from the pyrolysis of **1**[1k] and **7**.[3] On the other hand, 88% of **6** is predicted to be in the *E* form, again in agreement with its qualitative predominance in the IR spectra when generated by pyrolysis.[1p,8]

A small inherent preference for the *Z* conformation is indicated by the 0.3 kcal/mol preference for (*Z*)-**12**, the unsubstituted case, as well as the larger preferences for (*Z*)-**3** and (*Z*)-**8**. Steric congestion between the two methyl groups in the *Z* form of methyl acetylketene ((*Z*)-**6**), which is relieved in the *E* conformation, has been suggested as the origin of the conformational preference for **6**.[1p] Structural evidence for steric congestion would be expected

(6) Reed, A. E.; Curtiss, L. A.; Weinhold, F. *Chem. Rev.* **1988**, *88*, 899–926.

(7) Breneman, C. M.; Wiberg, K. B. *J. Comput. Chem.* **1990**, *11*, 361–373.

(8) The exact ratio of *Z* to *E* cannot be directly obtained from the IR spectra because there may be differences in the absolute intensities of the absorption bands of the conformations. The calculated infrared intensities provide a more accurate estimate of the experimental ratio, as discussed below in the context of the IR spectra.

Table 4. Atomic Charges of Acetylketene and Derivatives[a]

atom no.	3						6						8					
	Z			E			Z			E			Z			E		
O_1	−0.39[b]	(−0.50)[c]	[−0.59][d]	−0.40	(−0.52)	[−0.56]	−0.40	(−0.51)	[0.64]	−0.41	(−0.52)	[−0.61]	−0.37	(0.48)	[−0.58]	−0.38	(−0.49)	[−0.57]
C_2	0.61	(0.95)	[1.17]	0.55	(0.89)	[1.04]	0.58	(0.95)	[1.20]	0.51	(0.89)	[1.07]	0.65	(0.94)	[1.06]	0.59	(0.88)	[0.96]
C_3	−0.44	(−0.74)	[−0.99]	−0.40	(−0.70)	[−0.93]	−0.30	(−0.51)	[−1.00]	−0.26	(−0.48)	[−0.90]	−0.43	(−0.51)	[−0.38]	−0.40	(−0.48)	[−0.30]
C_4	0.56	(0.68)	[0.87]	0.55	(0.67)	[0.96]	0.56	(0.69)	[0.89]	0.56	(0.68)	[0.90]	0.59	(0.67)	[0.60]	0.59	(0.66)	[0.71]
O_5	−0.57	(−0.67)	[−0.69]	−0.54	(−0.64)	[−0.70]	−0.57	(−0.67)	[−0.73]	−0.55	(−0.65)	[−0.67]	−0.56	(−0.66)	[−0.68]	−0.52	(−0.61)	[−0.61]
X_6[e]	0.20	(0.28)	[0.25]	0.22	(0.30)	[0.25]	−0.32	(−0.64)	[0.75]	−0.29	(−0.63)	[0.85]	0.06	(0.02)	[−0.15]	0.08	(0.04)	[−0.17]
C_7	−0.42	(−0.74)	[0.21]	−0.44	(−0.75)	[0.03]	−0.42	(−0.74)	[0.17]	−0.44	(−0.75)	[0.16]	−0.42	(−0.74)	[0.60]	−0.44	(−0.75)	[0.26]
H_8[f]	0.14	(0.24)	[−0.07]	0.14	(0.24)	[−0.01]	0.14	(0.24)	[−0.04]	0.15	(0.24)	[−0.06]	0.16	(0.25)	[−0.15]	0.15	(0.24)	[−0.09]
H_9	0.16	(0.25)	[−0.10]	0.17	(0.26)	[−0.05]	0.17	(0.25)	[−0.11]	0.17	(0.26)	[−0.1]	0.17	(0.26)	[−0.20]	0.18	(0.26)	[−0.11]
H_{10}[f]							0.14	(0.24)	[−0.17]	0.15	(0.24)	[−0.17]						
H_{11}							0.14	(0.24)	[−0.17]	0.12	(0.23)	[−0.22]						

[a] Calculated at the RHF/6-31G**//RHF/6-31G* level. [b] Mulliken charges. [c] Natural bond orbital charges, in parentheses. [d] CHELPG charges, in brackets. [e] In 3, X = H; in 6, X = C; in 8, X = Cl. [f] CHELPG gave different charges for these sets of two symmetrically equivalent hydrogens.

and is manifest in the geometry of (*Z*)-6 (see Table 1 and Figure 1). The most dramatic distortions are seen in the C_4–C_3–C_6 angles. In (*Z*)-6, this angle is 6.1° wider than in (*E*)-6 in order to accommodate the two bulky methyl groups. The C_2–C_3–C_4 angle is compressed by 5.4° in (*Z*)-6 relative to (*E*)-6 to compensate. This distortion can also be seen in the C_4–H_{10} distance, which is 0.129 Å longer in (*Z*)-6 than in (*E*)-6. Comparison of acetylketene (3) with methylacetylketene (6) provides another perspective on the same distortion. The C_2–C_3–$C_6(H_6)$ angle is wider in 6 as compared to 3, 2.2° more open in (*Z*)-6 than in (*Z*)-3, and 3.3° more open in (*E*)-6 than in (*E*)-3. This suggests there is some repulsion between the C_6 methyl group of (*Z*)-6 and the ketene. However the repulsion between the two methyl groups also opens the C_4–C_3–C_6 angle in (*Z*)-6 1.7° wider than in (*Z*)-3. The changes at the ketone end of the molecules are smaller but are also consistent with steric crowding. The C_3–C_4–C_7 angles in (*E*)-3 and (*E*)-6 are quite similar, with (*E*)-6 only 0.7° wider. However, this angle is 1.8° larger in (*Z*)-6 than in (*Z*)-3. In all these comparisons the geometrical distortions are consistent with the proposal that steric interactions destabilize (*Z*)-acetylketene ((*Z*)-6).

Steric hindrance would also be expected to play a role in the conformational preference of chloroacetylketene ((*Z*)-8), although other factors may also be important. The C_4–C_3–Cl_6 angle in (*Z*)-8 is 124.9°, which is larger than the C_4–C_3–H_6 angle in (*Z*)-3 (124.0°) but smaller than the C_4–C_3–C_6 angle of (*Z*)-6 (125.7°). This suggests that the steric hindrance is intermediate between that in 3 and 6. However, the C_3–C_4–C_7 angles do not follow quite such a tidy trend when (*Z*)-8 is included. At 118.0° in (*Z*)-8, this angle is larger than that in (*Z*)-3, which is 115.8°, but it is also larger than that in (*Z*)-6, 117.0°. While it appears not possible to directly compare steric hindrance in (*Z*)-6 and in (*Z*)-8, in both molecules it provides a bias toward the *E* conformation as compared to the unsubstituted case ((*Z*)-3).

The question remains, then, as to the origin of the intrinsic preference for the *Z* conformation which is manifest in the relative stability of (*Z*)-3,[1k] (*Z*)-8,[3] and (*Z*)-formylketene (12).[2b,d] In the gas phase, molecules tend to adopt conformations in which their molecular dipole moments are minimized.[9] This cannot be the origin of the preference in this case, however. In the *Z* forms of 3, 6, 8, and 12, the dipoles of the ketene and carbonyl moieties are roughly parallel, reinforcing each other, while in the *E* forms, these group dipoles are roughly antiparallel. This results in significantly higher dipole moments for the *Z* forms of 3 and 6, as shown in Table 2.

The geometries provide an indication of the origin of the stabilization of the *Z* forms. In (*E*)-3, the C_2–C_3–C_4 angle is 5.0° larger than in (*Z*)-3. Nguyen et al.[2b] find a similar, but less pronounced, trend in formylketene (12), where the angle is 1.8° larger in the *E* conformation than the *Z*. Taken together, these suggest both a repulsive interaction between the methyl group (C_7) and the ketene (C_2) and an attractive interaction between the ketene (C_2) and the carbonyl oxygen (O_5) in (*Z*)-3. In-plane orbital overlap between the central ketene carbon and the carbonyl oxygen, which will be referred to as the covalent model, could be suggested to be the attractive interaction which stabilizes the *Z* form. This may be viewed as either a resonance contribution from or a mixing of states which includes the antiaromatic and highly strained ring-closed isomer 13 as shown in eq 2. It predicts specific changes in

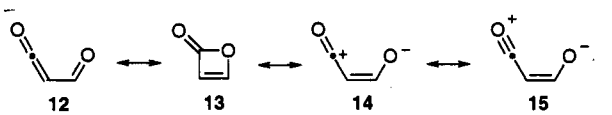

2

bond angles and distances between the *Z* and *E* conformations. In the *Z* forms, the C_2–C_3 and C_4–O_5 distances should be longer than in the *E* forms, and the C_3–C_4 distance should be shorter. The very small calculated distortions are in agreement with this prediction. For example, in acetylketene (3) the C_2–C_3 and C_4–O_5 bonds are slightly longer in the *Z* form (0.006 Å and 0.004 Å, respectively) than in the *E* form. The C_3–C_4 distance is 0.005 Å shorter in (*Z*)-3 than in (*E*)-3. Similar small differences in these bond lengths are observed between the *Z* and *E* forms of 6 and 8 as well. Bonding in the *Z* conformation should also bring C_2 and O_5 closer together, which would be manifest in smaller bond angles in the ring. The C_2–C_3–C_4 angle is indeed 5.0° smaller in (*Z*)-3 than in (*E*)-3 but the C_3–C_4–O_5 angle is 1.8° larger in (*Z*)-3 than in (*E*)-3. The latter is not primarily due to steric crowding between the methyl group and the ketene in (*E*)-3; Nguyen et al. report that this bond angle in formylketene is also larger in the *Z* conformation.[2b] Thus, the opening of the C_3–C_4–O_5 angle in (*Z*)-3 is not consistent with the covalent model. However, it is consistent with a change from a ketone toward an enolate, as expected from the electrostatic model described below. The HCO bond angle in formaldehyde is calculated to be 122.2° at

(9) (a) Wennerstrom, H.; Forsend, S.; Roos, B. *J. Phys. Chem.* **1972**, *76*, 2430. (b) Wang, X.; Houk, K. N. *J. Am. Chem. Soc.* **1988**, *110*, 1870–1872. (c) Wiberg, K. B.; Laidig, K. E. *J. Am. Chem. Soc* **1988**, *110*, 1872–1874.

the RHF/6-31G* level,[10] which is smaller than the CCO bond angle of 131.3° in the enolate of acetaldehyde calculated at the same level.[11] The ketene moiety would also be expected to bend if it is undergoing rehybridization, and this is also found to a very minor extent. The calculated geometries of the *Z* forms of **3**, **6**, and **8** all show a small bend of less than 1.5° away from the carbonyl as compared to the *E* forms. However, participation of **13** in the bonding scheme also implies that the O_1–C_2 distance should be longer in the *Z* conformation where there is a contribution from a lactone carbonyl than in the *E* where it remains a ketene. This is not found. Rather, this distance is slightly shorter in all the *Z* conformations. In (*Z*)-**3** the O_1–C_2 distance is 1.133 Å, which is 0.005 Å shorter than in (*E*)-**3**. Furthermore, calculations from this laboratory[2d] and by others[2b] have shown that the bonding in **13** is very weak, with a remarkably small barrier (2.5 kcal/mol at the MP4/(SDQ)/6-31G*//MP2/6-31G* + ZPE level)[2d] for its ring opening to **12** via a pseudopericyclic pathway.

An alternative model which offers a more consistent explanation of the stability of the *Z* forms is based on the electrostatic interactions of the array of atomic charges. Qualitatively, the central carbon of the ketene functionality bears a partial positive charge and the carbonyl oxygen bears a partial negative charge, as in **14** (eq 2). The *Z* conformations bring these charges into close proximity and, thus, should be stabilized by the electrostatic attraction between these two centers. Conversely, the *E* conformations enforce a greater degree of charge separation and are therefore less stabilized. A quantitative description of this interaction might begin with values for the atomic charges in each conformation. There have been many approaches developed to define such charges[5,6,13] because they have been an extremely useful and intuitive concept for chemists. However, because they are not observables of the Hamiltonian, there has been much controversy surrounding these methods.[6h,14] In the absence of a single accepted method for assigning charges, Mulliken, natural bond orbital analysis (NBO)[5,6] and CHELPG atomic charges[7] were determined and are reported in Table 4. These were calculated at the RHF/6-31G**//RHF/6-31G* level. The 6-31G** basis set was used to better represent the charges on the hydrogens. Mulliken charges are determined from the orbital populations, while NBO charges are similarly determined from the natural orbital occupancies. CHELPG fits atomic charges to reproduce the electrostatic potential around the molecule.[6,13]

The Mulliken, NBO, and CHELPG methods all predict that the central ketene carbons (C_2) of **3**, **6**, and **8** bear the positive charge and the carbonyl oxygens (O_5) bear the negative charge required for the electrostatic interaction proposed above. The trends in the Mulliken and NBO charges closely parallel one another, in that the differences between charges in the *Z* and *E* conformations are nearly identical within the two models. The trends in the CHELPG charges differ somewhat. Significantly, the monopole charges predict a far greater stabilization of the *Z* conformations than is found by the *ab initio* calculations. If one simply calculates the electrostatic energy of the array of monopoles from the CHELPG method at the appropriate nuclear positions, then (*Z*)-**3** is stabilized by 57.4 kcal/mol relative to (*E*)-**3**. Similarly, (*Z*)-**6** is stabilized by 47.1 kcal/mol relative to (*E*)-**6** and (*Z*)-**8** by 96.5 kcal/mol relative to (*E*)-**8**. If the atomic charges for (*Z*)-**3** are used at both the *Z* and *E* geometries, then (*Z*)-**3** is still 6.9 kcal/mol more stable. This should not be construed as criticism of the CHELPG method *per se*; the method is designed for a different purpose, namely to reproduce the electrostatic potential around a molecule. It does, however, point out the need for methods of determining atomic charges which will reproduce electrostatic effects within a molecule as well as without.

The stability of the zwitterionic resonance structures **14** and **15** in the *Z* conformations should cause their contributions to increase in the *Z* relative to the *E* conformations. This should in turn increase the magnitude of the charges. The Mulliken and NBO charges do indeed increase in the *Z* forms as predicted by this electrostatic model. In (*Z*)-**3** the O_5 charge is 0.03 more negative than in (*E*)-**3** as calculated by both methods. Similarly, both predict that the positive charge on C_2 increases by 0.06 from (*E*)-**3** to (*Z*)-**3**. The trends for these charges are the same for the *Z* and *E* conformations of **6** and **8**.

The huge electrostatic stabilization of the *Z* conformations shows that the magnitude of the CHELPG charges increases in the *Z*. However, the details of these changes are not as straightforward to interpret. The negative charge on O_5 in (*Z*)-**3** is slightly more positive (0.01) than in (*E*)-**3** contrary to expectation.[15] However, the positive charge on C_4 in (*Z*)-**3** is reduced by 0.09 from (*E*)-**3**. Thus, there is a net transfer of electron density to the C_4–O_5 carbonyl in the *Z* conformation. The positive charge on C_2 is greater by 0.13 in (*Z*)-**3** as compared to (*E*)-**3**, as predicted by the electrostatic model. Similar trends are again found in **6** and **8**. The covalent model for the stability of the *Z* conformations with bonding between C_2 and O_5 in the *Z* implies that the C_4–O_5 carbonyl becomes more like a carbon–oxygen single bond and O_5 more like an ester oxygen. This should reduce the negative charge on O_5, in contrast to the increase observed.

The participation of zwitterionic resonance structures **14** and **15** should also be reflected in the bond lengths. As with the participation of resonance structure **13**, the C_2–C_3 and C_4–O_5 distances should be longer in the *Z* conformation than in the *E*, and the C_3–C_4 distance should be shorter. However, participation of **15** with an O_1–C_2 triple bond should lead to a shorter bond length, while participation of the ring resonance structure **13** with a

(10) Hehre, W. J.; Radom, L.; Schleyer, P. v. R.; Pople, J. A. *Ab Initio Molecular Orbital Theory*; John Wiley and Sons: New York, 1986.

(11) The geometry of this enolate has been calculated by a number of workers,[12] but apparently not at this level of theory.

(12) (a) Dahlke, G. D.; Kass, S. R. *J. Am. Chem. Soc.* **1991**, *113*, 5566–5573. (b) Smith, B. J.; Radom, L.; Kresge, A. J. *J. Am. Chem. Soc.* **1989**, *111*, 8297–8299.

(13) (a) Bader, R. F. W.; Tal, Y.; Anderson, S. G.; Nguyen-Dan, T. T. *Isr. J. Chem.* **1980**, *19*, 8–29. (b) Chirlian, L. E.; Francl, M. M. *J. Comput. Chem.* **1987**, *8*, 894. (c) Davis, M. E.; McCammon, J. A. *J. Comput. Chem.* **1990**, *11*, 401–409. (d) Williams, D. E. In *Reviews in Computational Chemistry*; Boyd, D., Lipkowitz, K., Eds.; Wiley Interscience: New York, 1991; pp 219–271. (e) Westbrook, J. D.; Levy, R. M.; Krogh-Jespersen, K. *J. Comput. Chem.* **1992**, *13*, 979–989. (f) Sokalski, W. A.; Shibata, M.; Ornstein, R. L.; Rein, R. *J. Comput. Chem.* **1992**, *13*, 883–887. (g) Su, Z. *J. Comput. Chem.* **1993**, *14*, 1036–1041. (h) Sokalski, W. A.; Keller, D. A.; Ornstein, R. L.; Rein, R. *J. Comput. Chem.* **1993**, *14*, 970–976.

(14) (a) Perrin, C. L. *J. Am. Chem. Soc.* **1991**, *113*, 2865. (b) Merz, K. M., Jr. *J. Comput. Chem.* **1992**, *13*, 749–767. (c) Stouch, T. R.; Williams, D. E. *J. Comput. Chem.* **1993**, *14*, 858–866. (d) Urban, J. J.; Famini, G. R. *J. Comput. Chem.* **1993**, *14*, 353–362.

(15) It may be that this anomaly results from the way in which the CHELPG algorithm computes the charge distribution on the carbonyl in the two conformations, due to differences in the grid point alignments.[7,13c,e,g,14c,d] This possibility was not explored further.

lactone carbonyl would make this distance longer. In (*Z*)-**3**, the O_1–C_2 distance is 1.133 Å which is slightly shorter (by 0.005 Å) than the 1.138 Å in (*E*)-**3**. This bond length is shorter in (*Z*)-**6** and in (*Z*)-**8** by 0.005 Å in both cases relative to (*E*)-**6** and (*E*)-**8**. The Mulliken and NBO charges (but not the CHELPG charges) also reflect resonance structure **15** in that the negative charge on O_1 is slightly reduced (0.01, Mulliken; 0.02 NBO) in (*Z*)-**3** relative to (*E*)-**3**.

The electrostatic model also provides a rationale for the greater potential energy preference for (*Z*)-**8**. The electrostatic potential of the array of charges predicts that (*Z*)-**8** is stabilized by 96.5 kcal/mol, much more than (*Z*)-**3** and (*Z*)-**6**. The electron-withdrawing chlorine also bears a partial negative charge, according to CHELPG and chemical intuition,[16] and in the *E* form it is close to O_5 which also bears a partial negative charge. The proximity of the two partial negative charges destabilizes (*E*)-**8**. The C_4–C_3–Cl_6 and C_3–C_4–O_5 bond angles are wider in (*E*)-**8** (120.6° and 120.7°) than in (*E*)-**6** (119.6° and 118.9°). While both structures may experience some steric repulsion, in (*E*)-**8** the larger angle bending suggests greater repulsion.

In summary, the electrostatic model is consistent with the calculated differences in atomic charges and changes in bond lengths and angles between the *Z* and *E* conformations of **3**, **6**, **8**, and **12**. The covalent model is consistent with most of the differences in bond lengths and angles, but not with all of them. The covalent model does not predict the calculated changes in the atomic charges between the two conformations while the electrostatic model does. As will be discussed below, the structural changes implied by the electrostatic model are also consistent with the observed differences in the infrared spectra of the *Z* and *E* conformers of **3**, **6**, **8**, and **12**.

Infrared Spectra. Because the spectroscopic identification of the α-oxo ketenes and the assignments of *Z* and *E* conformations are based primarily on the IR spectra, and in particular on the ketene and carbonyl stretches, we anticipated that comparison of the calculated and experimental spectra would provide additional insight into and support for the assignments. Thus, the experimental and calculated spectra will first be compared for these peaks. The calculation spectra suggest assignments for additional, unassigned peaks in the experimental spectra, which will then be discussed.

It is a well-known deficiency of Hartree–Fock theory that the calculated vibrational frequencies are generally too high, and it is common to scale them by a factor of 0.9 to bring them into closer agreement with experiment.[10,17] Because the IR spectra are central to this work, and because of the unusual bonding in the ketene functionality, the accuracy of vibrational frequency calculations for ketene was examined at various levels of theory. The vibrational frequencies were calculated for ketene at the MP2(full)/6-31G* level, and root mean square error as compared to the experimental frequencies[18] is 106 cm^{-1}. That error is reduced to 24 cm^{-1} with a scaling factor of only 0.945. (A full tabulation of ketene frequencies including the MP2/6-31G* values is presented in the supplementary material.) The error in the RHF/6-31G* frequencies is 197 cm^{-1}, which, after scaling by 0.90, is reduced to only 31 cm^{-1}. This accuracy is comparable to that obtained by scaling the DZ + P frequencies (29 cm^{-1}).[19] The scaled ketene stretch of 2140 cm^{-1} (RHF/6-31G*) is only 13 cm^{-1} below the experimental frequency of 2153 cm^{-1}. Therefore, in the following discussions, the RHF/6-31G* calculated vibrational frequencies have been scaled by the 0.9 factor.

The vibrational frequencies and intensities were calculated for the *Z* and *E* forms of **3**, **6**, **8**, and **12** at the RHF/6-31G* level of theory. In order to demonstrate the validity of these calculations, the MP2(full)/6-31G* frequencies and intensities of formylketene (**12**) were also calculated at the MP2(full)/6-31G* geometries previously reported.[2d] Those vibrations which are predicted to be infrared active and in the spectral range accessible to the matrix IR experiments are reported in Table 5. The

Table 5. Comparison between Calculated and Observed Infrared Absorptions for Selected Vibrations of Acetylketene and Derivatives[a]

Z		*E*	
calcd frequency[b]	obsd absorption[c]	calcd frequency[b]	obsd absorption[c]
Acetylketene (**3**)[d]			
1167 (81)	1222 (w)[e]	1005 (38)	*f*
1372 (126)	1344 (m)	1219 (179)	1248 (w)[e]
1408 (249)	1378 (s)	1361 (75)	*g*
		1398 (45)	1365 (w)
1764 (265)	1681 (s)	1785 (536)	1698 (s)
2151 (1196)	2143 (vs)	2135 (1128)	2133 (vs)
Methylacetylketene (**6**)[h]			
973 (52)	*i*	919 (5)	913 (vw)
1106 (30)	*i*	989 (37)	986 (w)
1258 (136)	*i*	1273 (235)	1281 (m)
1348 (103)	*i*	1398 (41)	1362 (w)
1400 (105)	*i*		
1488 (29)	*i*		
1751 (254)	1666 (w)	1774 (491)	1686 (s)
2134 (1225)	2131 (m)	2122 (1152)	2123 (vs)
Chloroacetylketene (**8**)[j]			
950 (30)	950 (m)[e]	898 (18)	885 (w)[e]
		1023 (32)	1015 (w)[e]
1202 (60)	1215 (m)[e]	1225 (163)	1235 (s)[e]
1303 (299)	1315 (vs)	1308 (77)	*k*
1401 (74)	1420 (m)[e,l]	1396 (28) *k*	
1761 (221)	1670 (s)	1801 (437)	1705 (s)
2160 (1168)	2145 (vs)	2146 (1112)	2139 (vs)

Z		*E*	
RHF/6-31G*	MP2/6-31G*[m]	RHF/6-31G*	MP2/6-31G*[m]
Formylketene (**12**)			
933 (39)	934 (40)	1079 (93)	1057 (31)
		1096 (83)	1096 (103)
1373 (254)	1352 (201)	1318 (36)	1284 (45)
1765 (352)	1648 (184)	1787 (643)	1659 (309)
2153 (1130)	2112 (581)	2142 (1171)	2105 (624)

[a] All calculated absorptions between 800 and 2400 cm^{-1} with intensities above 30 km/mol are included. [b] Calculated vibrational frequency (cm^{-1}), scaled by 0.90, and calculated infrared intensity (km/mol) in parentheses. [c] Experimental infrared absorption (cm^{-1}) and relative intensity. [d] In argon matrix, from ref 1l. [e] Tentative assignment. [f] This region not displayed in published experimental spectrum. [g] May be obscured by 1344 cm^{-1} absorption of (*Z*)-**3**. [h] In argon matrix, from reference 1p. [i] Due to the low percentage of the *Z* conformation in the matrix, no other absorptions were assigned. [j] In nitrogen matrix, from ref 3. [k] May be obscured under peaks due to (*Z*)-**8**. [l] Alternatively assigned to peaks at 1445 or 1440 cm^{-1}. [m] Scaled by 0.945.

(16) By all three methods, Cl_6 in **8** is calculated to be substantially less positive than H_6 in **3**.

(17) Hess, A. B., Jr.; Schaad, L. J.; Polavara, P. L. *J. Am. Chem. Soc.* **1984**, *106*, 4348.

(18) Duncan, J. L.; Ferguson, A. M.; Harper, J.; Tonge, K. H. *J. Mol. Spectr.* **1987**, *125*, 196–215.

(19) Allen, W. D.; Schaefer, H. F., III. *J. Chem. Phys.* **1987**, *87*, 7076–7096.

complete calculated spectra are reported in the supplementary material. As expected, reasonable agreement was found between the scaled *ab initio* and experimental IR spectra. The calculated spectra confirm the original assignment of *Z* and *E* forms of **3**[1k] and **6**[1p] which rest to a large degree on the expectation that the ketene stretch would be at higher frequency and the carbonyl stretch at lower frequency for the *Z* as opposed to the *E* forms. Pyrolysis of **1** gives the two conformers of acetylketene[1k] (**3**). The observed ketene stretch at 2143 cm^{-1} and the associated carbonyl stretch at 1681 cm^{-1} have been assigned to (*Z*)-**3** while the more closely spaced peaks at 2133 and 1698 cm^{-1} were assigned to (*E*)-**3**. The calculations reproduce this trend, with the (*Z*)-**3** stretches at 2151 and 1764 cm^{-1} and the (*E*)-**3** stretches at 2135 and 1785 cm^{-1}, respectively. The same trend is calculated for **12**, where the carbonyl and ketene peaks are more closely spaced in (*E*)-**12** ($\Delta\nu$ = 355 cm^{-1}) vs. (*Z*)-**12** ($\Delta\nu$ = 388 cm^{-1}) at the RHF/6-31G* level and at the MP2/6-31G* level ($\Delta\nu$ = 471 cm^{-1} versus $\Delta\nu$ = 491 cm^{-1}). This trend in the IR absorptions is consistent with the electrostatic model and the participation of resonance structure **15** which predicts that the ketene bond (O_1–C_2) is strengthened and the carbonyl bond (C_4–O_5) is weakened in (*Z*)-**3** relative to (*E*)-**3**. The covalent model predicts that both bonds should be weakened in the *Z* conformation.

A similar trend is found for **6**. Pyrolytic generation of methyl acetylketene (**6**) from methyl 2-methyl-3-oxobutanoate gives a major product with bands at 2123 (vs) and 1686 (s) cm^{-1}, which were assigned to the *E* form.[1p] A peak was also observed at , 2119 (m) cm^{-1}, which was attributed to matrix effects. This is the exclusive product obtained upon photolysis of **5** in an argon matrix. The calculated absorptions of (*E*)-**6** are at 2122 and 1774 cm^{-1}. The minor conformation of **6**, produced by pyrolysis, has not been thoroughly characterized because it has a much smaller population in the matrix. However, the calculated spectra support the assignment of the weak and more widely spaced 2131 and 1666 cm^{-1} absorptions to the *Z* form. The calculated bands at 2134 and 1751 cm^{-1} are again more widely spaced than for the *E* form, consistent with a resonance contribution from **15**.

Although the assignments of *Z* and *E* conformations have been made solely on the basis of the ketene and carboxyl stretches, the calculated spectra predict additional diagnostic bands in the fingerprint region of the spectra which may also be assigned to particular conformations of α-oxo ketenes. The cleanest of the published spectra for these species is for (*E*)-**6**, which is the sole IR active product from photolysis of **6**.[1p] These calculations predict only three significant absorptions (calculated intensity greater than 30 km/mol) between 1700 and 700 cm^{-1}, at 1398 (w), 1273 (m), and 989 (w) cm^{-1}. These correspond well with the observed bands at 1362 (w), 1281 (m), and 986 (w) cm^{-1}. (These experimental intensities are based on inspection of the published spectra.) Wentrup also reports a (apparently very weak) band at 913 cm^{-1} which might correspond to the calculated one at 919 cm^{-1}. Because (*Z*)-**6** is only formed in a small proportion, the complete experimental spectrum is not available for comparison, but the locations and intensities of bands calculated for this species are clearly not compatible with those assigned above to the *E* conformation. The calculated spectrum of (*Z*)-**6** is predicted to have three closely spaced peaks of similar and moderate intensity at 1400, 1348, and 1258 cm^{-1} and weaker peaks at 1488, 1106, and 973 cm^{-1}.

Witzeman has kindly provided an unpublished spectrum of **8** produced by pyrolysis of **7**.[3] He has assigned the pairs of ketene and carbonyl absorptions at 2145 (vs) and 1670 (s) cm^{-1} and at 2139 (vs) and 1705 (s) cm^{-1} to the *Z* and *E* conformations, respectively, based, as usual, on the wider separation of peaks expected for the *Z* form. The calculations again reproduce this trend, with the absorptions of (*Z*)-**8** at 2160 and 1761 cm^{-1} more widely separated than those of (*E*)-**8** at 2146 and 1801 cm^{-1}. The carbonyl absorption of (*E*)-**8** is calculated to be twice as intense as that of (*Z*)-**8**. This is a consequence of the lower dipole moment of the *E* conformation as compared to the *Z* (vide infra), so that the carbonyl stretch leads to a greater change in the dipole moment. The intensity of the two carbonyl bands in the experimental spectrum are equal, which indicates that there is only half as much (*E*)-**8** as (*Z*)-**8** in the sample. With this in mind, the positions and intensities of the calculated bands allow preliminary assignments to be made for most of the experimental bands. The other absorptions in the experimental spectrum (excluding the acetone byproduct) are at approximately 1445 (m), 1440 (m), 1420 (m), 1360 (m), 1315 (vs), 1235 (s), 1215 (m), 1095 (w), 1020 (w), 1015 (w), 950 (m), 925 (w), and 885 (w) cm^{-1}. The very strong absorption at 1315 cm^{-1} must be due to the skeletal deformation calculated for the *Z* form at 1303 cm^{-1}, although there may be a small contribution to its intensity from the *E* band predicted to occur at 1308 cm^{-1}.

A peak of medium intensity is also predicted for (*Z*)-**8** at 1401 cm^{-1}, which presumably corresponds to one of the experimental peaks at 1445, 1440, or 1420 cm^{-1}. Another absorption is predicted at 1202 cm^{-1}, and one is found at 1215 cm^{-1}. A weak band is calculated at 950 cm^{-1}, and a band is indeed found at 950 cm^{-1}, although its intensity is slightly greater than calculated. Additional bands for the *E* conformation are predicted at 1396 (w), 1225 (m), 1023 (w), and 898 (w) cm^{-1}. Experimentally, the peaks found at 1235 (m), 1015 (w), and 885 (w) cm^{-1} may be assigned to the *E* form; the predicted band at 1396 cm^{-1} may be obscured or may be assigned to one of the bands at 1440 or 1420 cm^{-1}. The weaker experimental peaks at 1655, 1360, 1095, 1020, and 925 cm^{-1} are not assigned, but some may be due to unreacted starting material. These assignments are necessarily tentative, based as they are on a single spectrum. It is gratifying, nonetheless, that for each of the major calculated absorptions there is found a corresponding band in the experimental spectrum.

In the published spectrum containing (*Z*)-**3** and (*E*)-**3**, a band at 1378 (s) cm^{-1} was assigned to (*Z*)-**3**, but no other bands in the fingerprint region were assigned.[1k] This band corresponds in intensity and location to the calculated band at 1408 cm^{-1}. The other bands in the experimental spectrum are at 1365 (w), 1344 (m), 1248 (w), and 1222 (w) cm^{-1}. There is again twice as much (*Z*)-**3** as (*E*)-**3** in the sample because the experimental carbonyl bands are of equal intensity, while the calculated intensity of (*E*)-**3** is twice that of (*Z*)-**3**. On the basis, then, of both positions and intensities, the 1344 (m) cm^{-1} band corresponds to that calculated at 1372 cm^{-1} for (*E*)-**3**. There are two weak bands calculated for (*E*)-**3** in this vicinity, at 1398 and 1361 cm^{-1}. It seems most likely that the calculated band at 1398 cm^{-1} corresponds to that observed at 1365 cm^{-1}, while that calculated at 1361 cm^{-1} is obscured by the 1344

cm^{-1} band assigned to (*Z*)-**3**. The final two weak bands in the experimental spectrum, at 1248 and 1222 cm^{-1}, may be correlated with bands calculated at 1219 cm^{-1}, ((*E*)-**3**) and 1167 cm^{-1} ((*Z*)-**3**), respectively. The difference between the calculated and experimental peak locations is quite large, however, and so these assignments must be considered tentative. A more confident assignment of these smaller peaks awaits additional experimental data and/or higher level calculations.

The calculated intensities can be used not only to make assignments but also to quantify the proportions of *Z* and *E* present in spectra which contain both. Thus, the experimental peak heights of the ketene stretches of (*Z*)-**3** and (*E*)-**3**[1k] may be corrected for the differences in intensity predicted by the calculations. The relative intensities calculated at the RHF/6-31G* level for (*E*)-**12** and (*Z*)-**12** are almost the same as those from the MP2/6-31G* level, which indicates the reliability of the former. Correcting the experimental peaks by the calculated intensities indicates a slight predominance of (*Z*)-**3** (52%) formed by the pyrolysis of **1**. The similar correction for the carbonyl intensities of **8** is more substantial, and the results indicate the *Z* conformation accounts for 66% of the total population of **8**. Although the agreement is likely due in part to some cancellation of errors, these percentages are in remarkable agreement with the population calculated from the potential energies, zero-point energies, and entropies at the respective pyrolysis temperatures (see Table 3). The same calculations predict only 18% of (*Z*)-**6** to be formed by pyrolysis of methyl 2-methyl-3-oxobutanoate. Since the carbonyl stretch of (*E*)-**6** is calculated to be approximately twice the intensity of (*Z*)-**6**, (Table 5) it is not surprising that only a small amount of the latter is observed.[1p]

Conclusion

The geometries of the *Z* and *E* conformers of three substituted α-oxo ketenes (**3**, **6**, and **8**) have been calculated at the RHF/6-31G* level, and their relative energies have been compared at the MP4(SDQ)/6-31G*//RHF/6-31G* + ZPE level. Examination of similar calculations for formylketene (**12**) at the MP2/6-31G* optimized geometry indicates that the RHF/6-31G* level is adequate for the comparisons made here. The calculated infrared spectra reproduce the trends in ketene and carbonyl band location and separation observed experimentally. The calculated intensities permit quantification of the relative proportions of *Z* and *E* conformations observed, proportions which are closely reproduced by considering the potential energies, zero-point energies, and entropies from the calculations. As exemplified by formylketene (**12**), α-oxo ketenes exhibit an inherent preference for the *Z* conformation despite the fact that this conformation has a higher dipole moment. The *Z* preference is best explained by a model which considers the electrostatic attractions between the partially positive central carbon of the ketene (C_2) and the partially negative carbonyl oxygen (O_5). This model is consistent with both geometric and atomic charge differences calculated between the *E* and *Z* conformations and offers an explanation of trends in the carbonyl and ketene band positions in the IR spectra. Current procedures for the calculation of atomic charges are inadequate or inappropriate to quantify these electrostatic interactions, however. Steric effects in acetylketene (**3**) increase the preference for the *Z* conformation. On the other hand, entropy favors the *E* conformations, which along with steric congestion between bulky substituents can overcome the *Z* preference and lead to higher proportions of the *E* conformations, as in **6** and **11**.

Acknowledgment. It is a pleasure to thank J. Stewart Witzeman whose experimental studies provided the impetus for this work. The calculations were carried out using generous grants of computer time from Texas Tech University, the Pittsburgh Supercomputing Center, and Eastman Kodak Company at the National Center for Supercomputing Applications. Their support is gratefully acknowledged. Acknowledgment is make to the donors of the Petroleum Research Fund, administered by the American Chemical Society, for partial support of this work.

Supplementary Material Available: Tables of optimized *Z*-matrices for (*Z*)- and (*E*)-**3**, **6**, and **8** and ketene and of vibrational frequencies and intensities for (*Z*)- and (*E*)-**3**, **6**, **8**, and **12** and a comparison of calculated and experimental vibrational frequencies for ketene (9 pages). This material is contained in libraries on microfiche, immediately follows this article in the microfilm version of the journal, and can be ordered from the ACS; see any current masthead page for ordering information.